IOSR Journal of Applied Physics (IOSR-JAP)
e-ISSN: 2278-4861.Volume 8, Issue 2 Ver. I (Mar. - Apr. 2016), PP 87-94
www.iosrjournals.org

Verification of a Developed Automatic Counting System for Cr-39 Detectors Using Different Image Resolutions

M. Alssabbagh[1], B. Z. Shakhreet[2]
[1] *Advanced Medical and Dental Institute, Universiti Sains Malaysia, Bertam 13200 Kepala Batas, Pulau Pinang, Malaysia.*
[2] *Department of Diagnostic Radiology, Faculty of Applied Medical Sciences, King Abdulaziz University, P.O. Box 80324, Jeddah 21589, Saudi Arabia.*

Abstract : *This study is an extended research done by the research team based on their recently published research. The aim of this study is to verify a system software that was developed and verified using only one digital microscope with high specification as described in the previously published research, which automatically counts and characterizes ion tracks of irradiated CR-39 to alpha particles, by comparing the output images that were obtained from two different digital microscope models with different specifications.*
In this current research, two microscopes are used to capture the images of the detectors. The first one is a traditional light microscope with a digital camera connected to the eyepiece. The second microscope is a fully digital one with an LCD monitor with an area of 3.5" which acts as a 10x eyepiece. Two image resolutions of 0.3 Megapixels from the first microscope and 2.0 Megapixels from the second one are used. The same magnification is used for both microscopes. The manual counting is then compared with the automatic counting in both output images from both different microscopes. The automatic system was compared to the manual counting method for verification; it was found that low illumination uniformity of the images from one of the microscopes reduced the number of counted tracks, whilst good distribution of illumination from the other microscope promoted counting (both manual and automatic). Thence, it can be concluded that the system is highly dependent on image clearness. Additionally, the system showed the ability to count the tracks on different resolutions.

Keywords: *CR-39, Solid states nuclear track detectors, Microscope, Auto tracks counting*

I. Introduction

Solid state nuclear track detectors (SSNTDs) are a solid substance (plastic, glass or crystal) used for the detection of etched tracks formed due to the interaction of charged particles and neutrons inside this material. These detectors are usually insensitive to beta or gamma radiation. Many types of SSNTDs are available with varying sensitivities, such as polycarbonates, polyallyl diglycol carbonate and cellulose nitrates also known as MKE, CR-39 and CN-85 or LR-115 respectively [1].

As a non-volatile material, SSNTD can retain the tracks indefinitely due to being unaffected by temperature variations, light and humidity and they work as passive detectors where external energy is not necessary. In addition, they are inexpensive, robust and insensitive to electromagnetic waves as well [2, 3].
Due to these advantages they have many applications such as radon concentration measurements in houses and mines, studies on cosmic rays, and dosimetry in nuclear power plants. These are in addition to their applications in radiotherapy facilities and geology where they are used for earthquake prediction and volcanic surveillance [2, 4].

The tracks are initially too small to be visible under traditional light microscopes. The tracks are made visible using a suitable chemical etchant solution, usually sodium hydroxide (NaOH) or potassium hydroxide (KOH). Etching solutions enlarge the diameter of the tracks so that it can be seen under a traditional light microscope.

Counting the tracks on such detectors is difficult due to many factors, such as artifact degradations, overlapping of tracks and the size of the tracks which depends on the energy of the incident particles, the concentration of the chemical solution and the etching time [5].

Over the last few years, the CR-39 track detector has become a popular method to measure charged particles and neutrons. As the use of CR-39 detectors increased, the number of computerized track-counting systems has also increased.

The main target of this study was to verify the system software, which automatically counts and characterizes ion tracks of irradiated CR-39 to alpha particles by comparing the output images that are obtained from two different digital microscope models with different specifications. This software was developed and verified using only one digital microscope with high specification [6].

II. Literature

The CR-39 detector is very sensitive to charged particles and can record both protons and fast neutrons that have tracks of wide energy, ranging from several eVs to tens of MeV [2, 7]. The CR-39, as a passive detector, has the advantages of being an inexpensive, durable and transparent material that interacts with charged particles and neutrons, whilst not being sensitive to gamma, beta and electromagnetic radiation.

These particles ionize the detector along the track that they pass. This ionization process will create free radicals which cause damage inside the detector in the form of a "latent track". These tracks having diameters of less than 1 μm cannot be observed with the traditional light microscope [8]; therefore, a process called track etching or track visualization is carried out by exposing the detector to chemicals which etch the detector's surface and the pits resulting from the charged particles. This makes them larger, so they can then be seen using a conventional light microscope. This etching effect is called the "track effect" [9].

Throughout this project a number of CR-39 detectors were irradiated to a radon source, the radon concentration was determined and related to the track density (track per area). The calibration of these detectors was performed by exposing them to a known concentration of radon, then constructing a calibration curve to be used as a reference for the radon concentration in future unknown samples [10].

In general, one of the disadvantages of the CR-39 is that it has some background radiation caused by radon particles in the air as well as the backgrounds' artifacts, such as blebs and scratches on the detector's surface which become clearer with an etching process.

Most of the real tracks have higher OD (darker colors) in comparison to the defects, as shown in Figure 1. This can be used in the automatic system, by converting the image to binary mode and entering a binary threshold to eliminate the defects.

In general, the angle of incident particles will determine whether the tracks will appear on the detector or not, and will identify the tracks' shape (circular or elliptical) as shown in Figure 1. It is shown that the artifacts are similar to the tracks but with different OD. The different sizes of real tracks are caused by different particle energies.

The track diameter can be affected by the energy of the incident particle; higher energies will increase the diameter of the fully etched track. Thus, the energy loss per unit path (dE/dx) decreases with higher energies due to the increase in the penetration and the short interaction time [2], where dx is the penetrating distance and dE is the mean energy of the particles being transferred to the material [9]. Short etching times may not cause all the tracks to show or will have small diameters even at high energies.

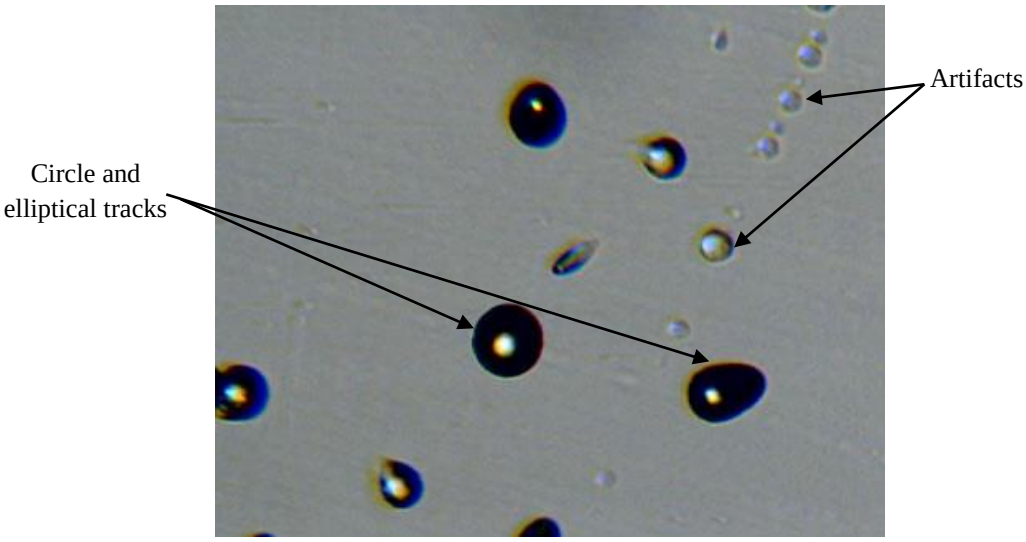

Fig. 1 Image of a detector having circular tracks, elliptical tracks and defects.

Image processing is used in many developed automatic counting software to improve the output image to get the tracks counted. One of the image processing methods is restoration, which is demonstrated in Figure 2. The input image $f(x,y)$ has several kinds of degradations; the function $g(x,y)$ and other corrections are applied on this image in order to produce the enhanced output image $\hat{f}(x,y)$.

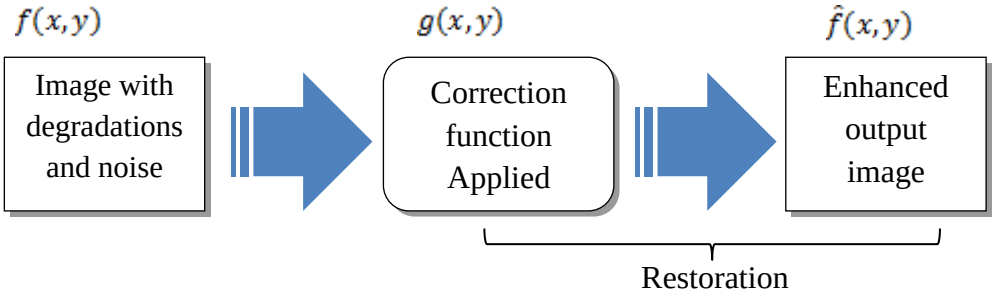

Fig. 2 Diagram illustrating the restoration model

It was assumed that these defects were considered as noise with the absence of any other degradation factor such as motion blurring.

The characteristics of the tracks mentioned above were used to build a system to count the tracks depending on the size, optical density and circularity thresholds.

Many researchers used the same etchant chemicals and etching process as well as the same detectors and irradiating conditions. Many Automatic counting systems have been introduced [6]. They used either their own developed software or commercial software packages such as Image-Pro v.4.0 or free downloadable Image-J software.

Most of those systems were counting the tracks and ignoring the overlapped ones.

An interesting program called TRACK II created by Patiris, Blekas, & Ioannides (2007) using MATLAB® depends significantly on the track radius, brightness and track orientation. One of this program's features is counting the overlapped tracks using the Hough transform to find the strongest peak in the overlapped shape (which is either circular or elliptical); the number of these peaks represents the number of overlapped tracks. This is very time-consuming as at each overlap the strongest peak must be found; Figure 3 demonstrates this method.

The concept of analyzing the images using this software is that each data point has a pixel intensity value depending on an algorithm called the K-means that minimizes the intensity from the data points in the image to their closest center; it depends on the number of clusters available which must be entered by the user. The user must also enter a size threshold, where objects having sizes less than this threshold are not taken into consideration.

The current study aims to show that the developed automatic counting system that was tested and verified using only one high-specification digital microscope by M. Alssabbagh and B. Z. Shakhreet (2016) can detect and count the tracks on two different image resolutions taken by different microscopes.

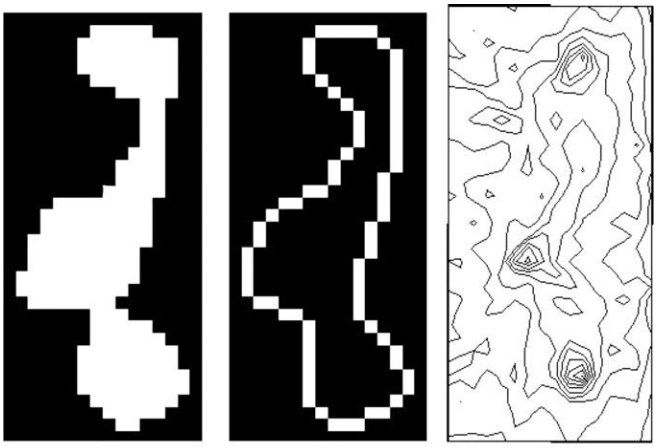

Fig. 3 The strongest peak in the overlapped tracks. "(a) An object composed of three overlapped tracks. (b) An estimation of the object's edges. (c) The Hough transform detects three tracks, as the accumulator function has 3 major peaks" [11].

III. Methodology

The same CR-39 detectors that were used by M. Alssabbagh and B. Z. Shakhreet (2016) were used in this study. The tracks that resulted from radon particles were counted manually and then compared to the results produced by the automatic counting system for validation purposes. Two microscopes with digital cameras were

used to capture the images of the detectors. The first one was a traditional light microscope with a digital camera connected to the eye piece with an image resolution of 0.3 Megapixels. The second microscope is the same one that was used by M. Alssabbagh and B. Z. Shakhreet (2016) which has an image resolution of 2.0 Megapixels.

The magnification used in the first microscope was 40X with a scene area of 0.0038 cm^2 and a resolution of 640 × 480, while the second one is also 40X with a scene area of 0.013 cm^2 and a resolution of 800 × 600. The second microscope has a larger scene area than the first one. A new set of images is taken by the first microscope, where manual and automatic counting were performed for the images taken from both microscopes.

By measuring the pixelated size of tracks in the new images, they were found to have relatively the same values to those of the images taken by the second microscope (2.0 Megapixels), as well as that they have the same zoom magnification. The threshold size is fixed and unaltered.

Similarly, in this study, the same procedure that was applied by M. Alssabbagh and B. Z. Shakhreet (2016) to count the tracks manually and automatically from the images of both microscopes was adopted. For the automatic counting, the same thresholds (binary, size and circularity) were applied.

The total area of the 20 pictures (scenes) that was captured for each individual detector from the first and second microscopes is 0.076 cm^2 and 0.26 cm^2 respectively.

To calculate the concentration (density) of tracks on each detector, the following equation is applied:

$$D = \frac{N \pm \sqrt{N}}{A} \tag{1}$$

where D is the track density on the detector (Tr/cm^2), N is the total number of counted tracks from all scenes after subtraction of the background and A is the scene area of all scenes (cm^2). The square root of the total tracks $\sqrt{N}$ is equal to the error of these tracks [2].

The calibration curves are then plotted for manual and automatic counting of the images from each microscope.

IV. Results and Discussion

This system was used for two different images resolutions. The first type of images had 0.3 Megapixels for the first microscope while the second type of images had 2.0 Megapixels for the second microscope. The standard radon cell of 700 litters in the Syrian Atomic Energy Commission was used to measure the radon activity in the air. A stable concentration of radon in the standard radon cell is reached after equilibrium; this is equaled to 170 KBq/m^3. The concentration of radon inside the cell is then measured from different period times (1, 2, 4, 8 and 13 hours).

The most important factor affecting the clearness of the images is the illumination. A significant number of real tracks were lost in the images taken by the first microscope when adjusting the binary threshold, due to the increased size of black edges which result from the non-uniform distribution of the microscope's illumination, making the track detection difficult both manually and automatically.

Figure 4-a shows that the black edges are graded from outside to inside (the images taken by the first microscope), while in Figure 4-b (the images taken by the second microscope) the illumination was distributed uniformly.

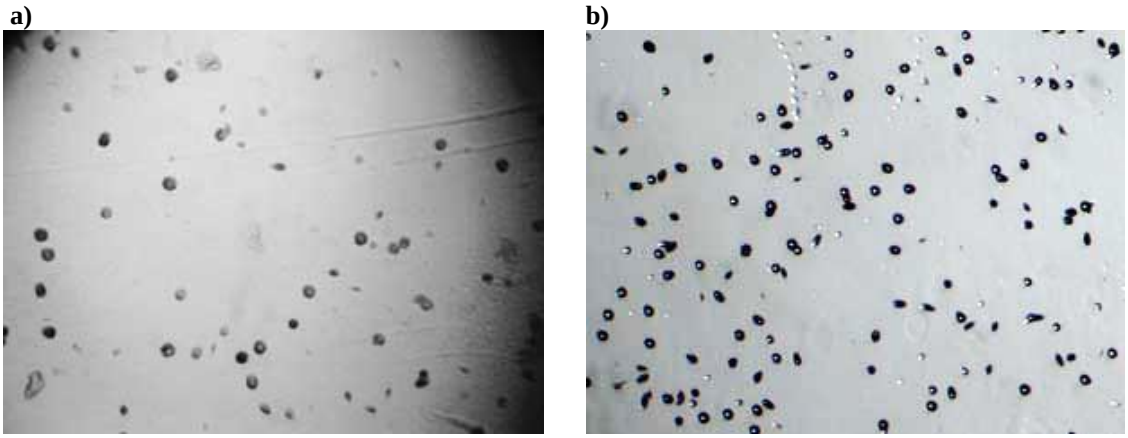

Fig. 4 Tracks as appeared from the two microscopes.

When reducing the binary threshold, the gradient edges became black, as seen in Figures 5 and 6 from both microscopes; covering the tracks under them which in turn led to a reduction in the number of counted tracks. It is illustrated in Figure 5 that the usage of different threshold values will have an effect on the track appearance. The reducing threshold will mask more tracks especially the ones near to the edges while increasing the threshold will cause the tracks to fade, especially the small ones. The chosen thresholds are 90, 130 and 160 for the images a, b and c respectively.

On the other hand, Figure 6 shows that the clearness of the taken image and usage of a suitable threshold value will affect the counted tracks. As it can be noticed here, image (c) is the best choice. The chosen binary thresholds are 90, 130 and 160 for the images a, b and c respectively.

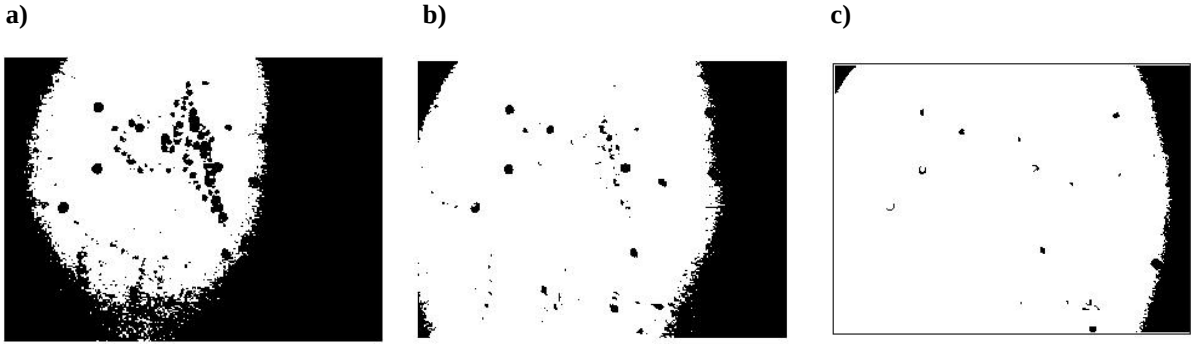

Fig. 5 Binary threshold on the gray-level images from the first microscope with black edges.

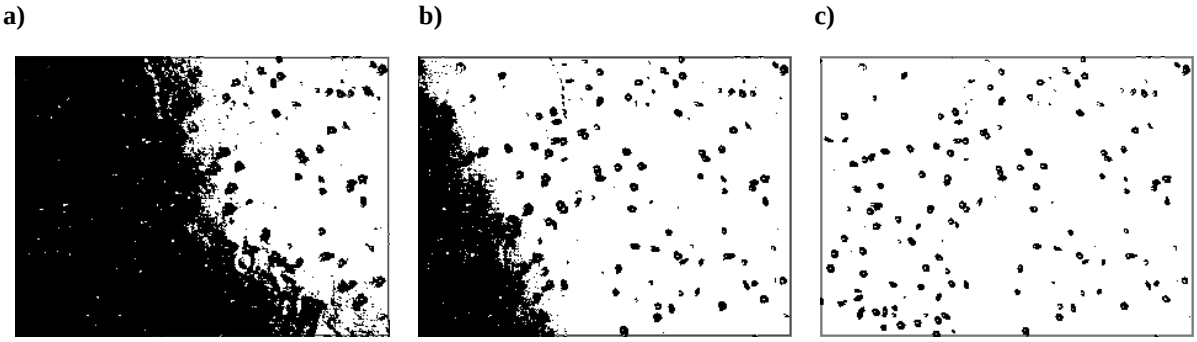

Fig. 6 Binary threshold on an image from the second microscope with no black edges.

The track concentrations of manual and automatic counting from the first microscope (0.3 Megapixels) were tabulated in Table 1. The number of tracks counted automatically dropped sharply compared to those counted manually, particularly for the detectors with high exposure times. This is due to a loss of a large amount of tracks which were masked under the black edges during automatic counting. The observer could manually differentiate the tracks in the graded black area in the grayscale image but at the cost of counting time.

Table 1 The tracks concentration of manual and automatically counted tracks on each detector from the first microscope.

Exposure time (hr)	**Manual Counting** **Track density ± Error** ($Tr.Cm^{-2}$)	**Automatic Counting** **Track density ± Error** ($Tr.Cm^{-2}$)	**Radon Exp. kBq.h/m^3** (standard radon cell)
1	973 ± 113	1434 ± 131	170
2	1671 ± 148	2421 ± 174	340
4	3052 ± 200	3789 ± 219	680
8	5434 ± 267	6144 ± 281	1360
13	9157 ± 347	868 ± 99	2210

As seen in the calibration curves of the manual and automatic counting of the first microscopes' images (Figures 7 and 8), the manual counting is more precise than the automatic one due to the poor clarity of the images. The slopes for both figures represent the calibration coefficient. The detected track using the manual method depends on the user's vision but at the expense of time (approximately 20 - 30 min. for each detector) and human error. In contrast, the automatic method is not time-consuming at all (~40 seconds for each detector),

but it is at the expense of the precision of the counted tracks. The decrease in the number of counted tracks is due to the images not being clear which results in a low calibration coefficient (2.89 compared to 4.15 for manual counting).

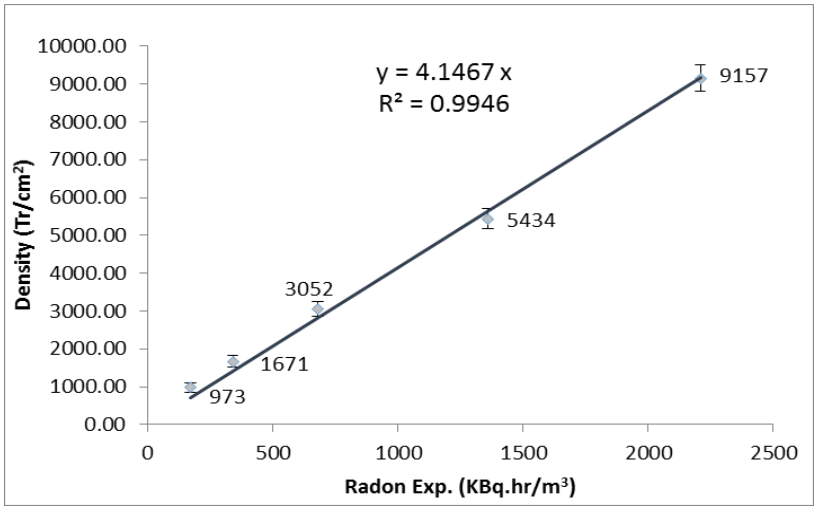

Fig. 7 Calibration curve for manual counting.

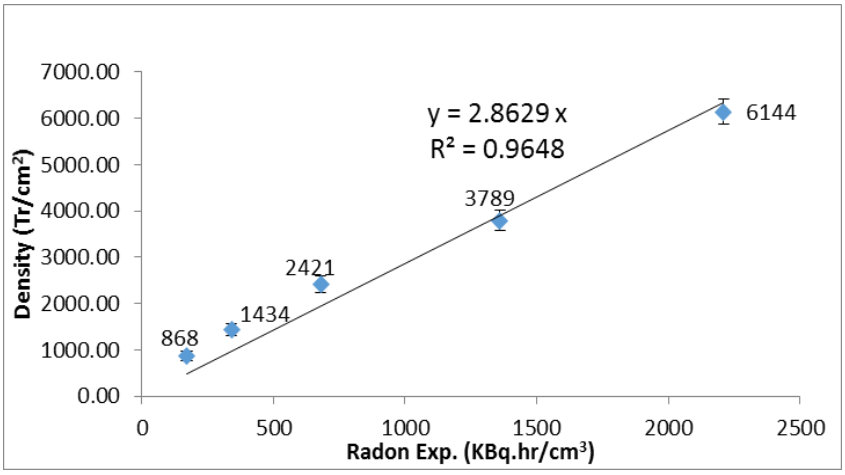

Fig. 8 Calibration curve for automatic counting.

Compared to the set of images taken by the second microscope (2.0 Megapixels), the manual and automatic counting are significantly enhanced. Table 2 shows the increase in track counts using manual counting; approximately the same numbers were obtained by the automatic system. This may indicate the superiority of natively digital microscopes versus traditional optical microscopes with a digitizer attachment; whereas the second one is lower in price and easier to use. The calibration curves from the second microscope can be seen in Figures 9 and 10, which show very similar calibration coefficients from both methods (4.65 for manual counting and 4.61 for automatic counting).

Table 2. The tracks concentration of each detector using the second microscope.

Exposure time (hr)	**Manual Counting** **Track density ± Error** ($Tr.Cm^{-2}$)	**Automatic Counting** **Track density ± Error** ($Tr.Cm^{-2}$)	**Radon Exp. kBq.h/m³** (standard radon cell)
1	516 ± 152	550 ± 157	170
2	1094 ± 222	1124 ± 225	340
4	2976 ± 367	2927 ± 363	680
8	5857 ± 514	5857 ± 514	1360
13	10713 ± 599	10602 ± 692	2210

It is clear from both the manual and automated results from both microscopes that the number of tracks counted is affected significantly by the clarity of the image, hence, the lower the number of counted tracks the higher the error.

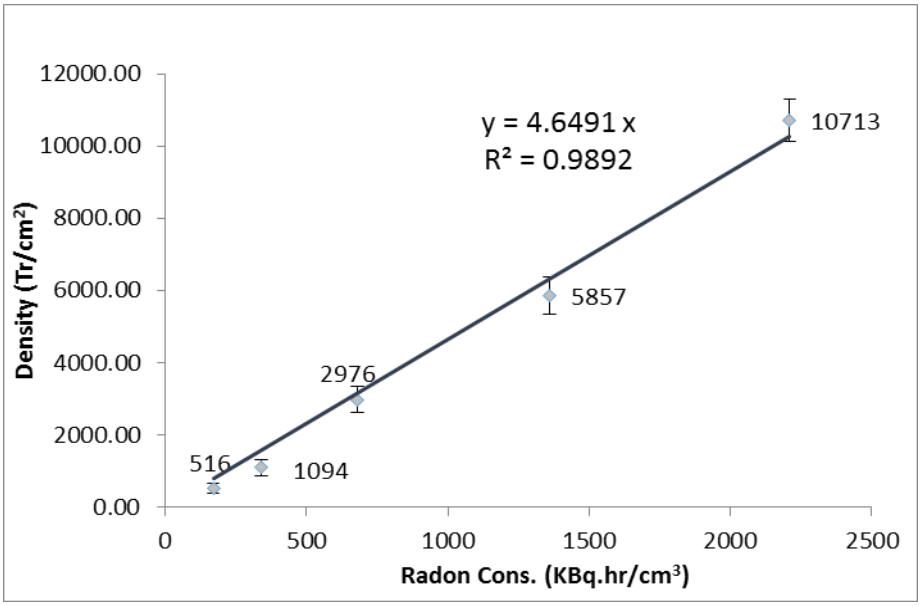

Fig. 9 Manual track counting calibration curve (using the new microscope).

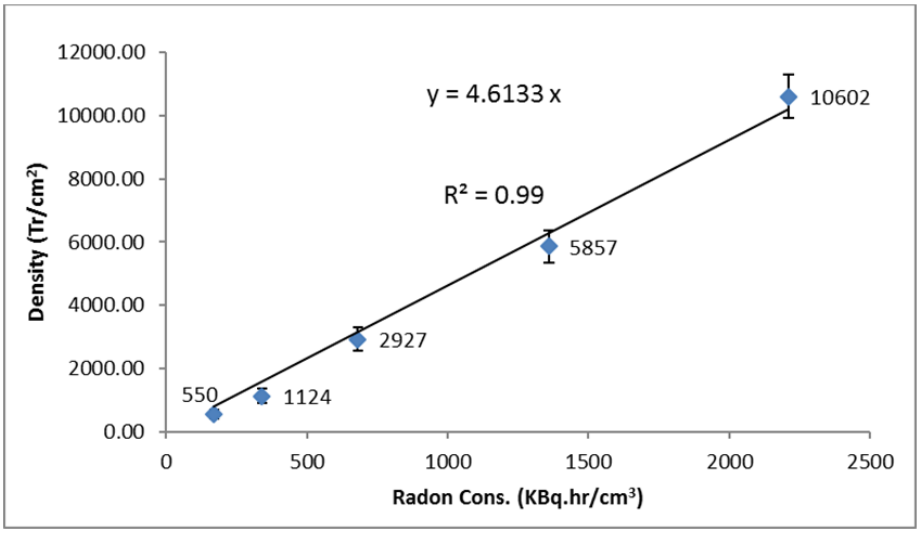

Fig. 10 Automatic track counting calibration curve (using the new microscope).

From the graphs in Figures 7, 8, 9 and 10 of manual and automatic counting for the images resulting from both the first and second microscope, it is observed that the relationship between radon exposure and track density is linear.

V. Conclusion

This system was used on two different image resolutions. A resolution of 0.3 Megapixels was used for the images of the first microscope and 2.0 Megapixels for the images of the second microscope. The system showed the ability to count the tracks on both resolutions.

The weakness of illumination uniformity in the first images influenced the number of counted tracks. Meanwhile, in the second images, the good distribution of the illumination promoted the counting in the two methods, namely the manual and automatic counting. Therefore, the system is highly dependent on the clarity or clearness of the image.

Acknowledgements

Many sincere thanks to Dr. Riad Shweikani, director of department of protection and safety in atomic energy commission of Syria,for his technical assistance and Dr. Ung Ngie Min (University of Malaya) for his recommendations that helped improve this study.

References

[1]. Puglies, F., Sciani, V., Stanojev Pereira, M. A. and Pugliesi, R. 'Digital System to Characterize Solid State Nuclear Track Detectors', Brazilian Journal of Physics, 37(2A), 2007, pp. 446-449.
[2]. Durrani, S. A. and Radomir, I. Radon Measurements by Etched track Detectors, Singapore: World Scientific Pub. Co. Pte. Ltd 1997.
[3]. AL-Talbany, N. F., Jaafar, S. M. and Al-Nafiey, M. S. Measurement the Concentration of Alpha Emitters in the Urine In Vitro, Natural Exposure, Journal of Natural Sciences Research, 3(3), 2013, pp. 62-68.
[4]. Sidorov, M. and Ivanov, O. Nuclear Track Detectors: Design, Methods and Applications, Nova Science Publishers, Inc. 2010, p. 275.
[5]. Choppin, G., Rydberg, J. and Liljenzin, J. O. Radiochemistry and Nuclear Chemistry, 3rd edition, Butterworth-Heinemann 2002, p. 709.
[6]. Alssabbagh, M. and Shakhreet B. Z. Developing a Fast Affordable Automatic Counting System of CR-39 Solid State Nuclear Track Detectors, Physical Science International Journal, 9(2), 2016, pp. 1-9.
[7]. Felice, P. D., Cotellessa, G., Capogni, M., Cardellini, F., Pagliari, M. and Sciocchetti, G. The Novel Track Recording Apparatus From Ssntd For Radon Measurement, Romanian Journal of Physics, 58, 2013, pp. S115-S125.
[8]. Gaillard, S., Fuchs, J., Galloudec, N. R.L. and Cowan, T. E. Study of saturation of CR39 nuclear track detectors at high ion fluence and of associated artifact patterns, Review of Scientific Instruments, 78(1), 2007, pp. 013304.
[9]. Nikezic, D. and K. N. Yu. Formation and growth of tracks in nuclear track materials, Materials Science and Engineering, 46, 2004, pp. 51-123.
[10]. Nikezic D., and K. N. Yu. Computer simulation of radon measurements with nuclear track detectors, Computer Physics Research Trends, 1st edition, Nova Science Publishers, Inc. 2007, pp. 119-150.
[11]. Patiris, D. L., Blekas, K. and Ioannides, K. G. TRIAC II. A MatLab code for track measurements from SSNT detectors, Computer Physics Communications, 177, 2007, pp. 329-338.
[12]. Ahn, G. H. and Lee, j.-k. Construction of an environmental radon monitoring system using cr-39 nuclear track detectors, nuclear engineering and technology, 37(4), 2005, pp. 395-400.
[13]. Zylstra, A. B., Frenje, J. A., Se´guin, GatuJohnson, F. H., Casey, M., D. T., Rosenberg M. J., et. Al. A new model to account for track overlap in CR-39 data, Nuclear Instruments and Methods in Physics Research A, 681, 2012, pp. 84-90.